Theory of hybrid state in a metal with a small Fermi surface and strong collective excitations

F. H. L. Essler[1] and A. M. Tsvelik[2]
[1]*Department of Physics, University of Oxford, 1 Keble Road, Oxford OX1 3NP, United Kingdom*
[2]*Department of Physics, Brookhaven National Laboratory, Upton, New York 11973-5000, USA*
(Received 29 September 2004; published 26 May 2005)

We develop a theory of a hybrid state, where quasiparticles coexist with strong collective modes, taking as a starting point a model of infinitely many one-dimensional Mott insulators weakly coupled by interchain tunneling. This state exists at an intermediate temperature range and undergoes an antiferromagnetic phase transition at temperatures much smaller than the Mott-Hubbard gap. The most peculiar feature of the hybrid state is that its Fermi surface volume is unrelated to the electron density. We present a self-consistent derivation of the low-energy effective action for our model.

DOI: 10.1103/PhysRevB.71.195116 PACS number(s): 71.10.Pm, 72.80.Sk

I. INTRODUCTION

The presence of strong collective modes interacting with quasiparticles is a distinctive feature of many strongly interacting systems such as "bad" metals, weakly doped Mott insulators (such as the cuprates), and heavy fermion materials. This interaction is believed to result in a variety of unusual phenomena observed in these systems, such as the violation of the Mott-Regel limit in the temperature dependence of the electrical resistivity of bad metals or the absence of quasiparticle peaks in the spectral function of the cuprates. The lack of nonperturbative techniques in dimensions higher than one makes a detailed theoretical description of these phenomena quite challenging. One successful approach has been developed by Chubukov, Schmalian, and Abanov, who have studied the so-called spin-fermion model put forward by Pines.[1] This model is semiphenomenological and postulates the existence of a strong, coherent, collective mode, which interacts with quasiparticles located in the vicinity of a Fermi surface. This model is reviewed comprehensively in Ref. 2 and has proven quite successful in explaining various properties of the cuprates. However, a derivation from a microscopic Hamiltonian is lacking.

In this paper we provide a microscopic derivation of a model in the same class as the spin-fermion models of Pines and Chubukov *et al.* Namely, we continue to develop a theory of a hybrid state combining the features of a Landau Fermi liquid and a Mott insulator suggested in Ref. 3. This state is characterized by the coexistence of well-developed collective modes with quasiparticles. The latter ones have a small Fermi surface (SFS), the volume of which is unrelated to the total number of electrons. By definition, the Fermi surface (FS) is small if its volume is less than the maximum volume allowed by Luttinger's theorem.[4–7] The existence of such a state does not contradict Luttinger's theorem, since the latter, contrary to popular belief, does not fix the volume of the FS. Instead the theorem states that the electron density n is proportional to the volume of phase space enclosed by the surface where the single-electron Green's function changes its sign,

$$n = \frac{2}{(2\pi)^d} \int_{G(\omega=0,\mathbf{k})>0} \mathrm{d}^d k. \tag{1}$$

When the Green's function has zeros, the Fermi surface constitutes only a part of this surface, namely, the one where $G(0,\mathbf{k}) \to \infty$. Hence Luttinger's theorem (1) does not even require the existence of a Fermi surface; the Green's function may have only zeros and no poles, as is the case for superconductors[5] and certain one-dimensional systems, in which the spectral gap is generated dynamically. (For the latter case a general proof is outlined in Ref. 8.)

A metallic state with a small FS would necessarily be associated with a Green's function that has both poles and zeros at $\omega=0$. In our previous work[3] we suggested a model for such a state based on the quasi-one-dimensional Hubbard model at half filling. The transverse hopping was treated in a random phase approximation (RPA). In order to understand the conditions of stability of such an exotic metal, one has to go beyond RPA, which is the main subject of the present paper. Experimental indications of the existence of the SFS states come from angle-resolved photoemission spectroscopy (ARPES) measurements in underdoped cuprates[9] and from the Hall-effect measurements in heavy fermion materials.[10]

Before turning to the calculations, we shall give a qualitative account of the physics we are after. Our starting point is an ensemble of uncoupled, Mott insulating chains. The relevant energy scale is the one-dimensional (1D) Mott gap m. We consider finite temperatures T such that $T \ll m$. The physics is purely one dimensional.

We then turn on a small long-range interchain tunneling with characteristic energy scale $t_\perp$. Clearly, at zero temperature the hopping between chains will be essential, and it will induce a three-dimensional (3D) ordered state. On the other hand, in the window,

$$t_\perp \ll T, \tilde{t}_\perp(\mathbf{k}) \ll m, \tag{2}$$

we will recover the physics of 1D Mott-insulating chains. Here $\tilde{t}_\perp(\mathbf{k})$ denotes the Fourier transform of the interchain tunneling. Furthermore, as $T \ll m$ we may, to a good approximation, work with zero-temperature quantities in many instances.

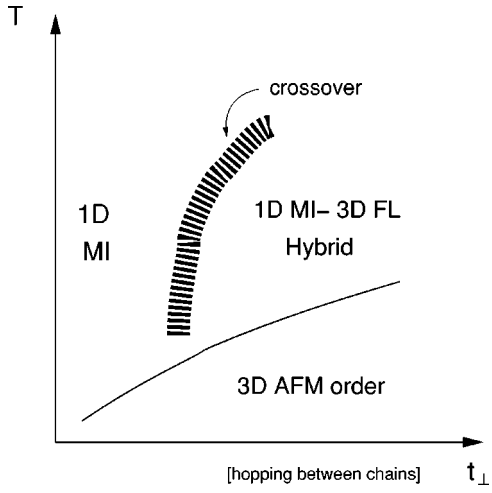

FIG. 1. Cartoon-phase diagram for $T \ll m$ for weakly coupled 1D Mott insulators, where m is the 1D Mott gap.

The crucial point is that while $t_\perp$ remains much smaller than the Mott gap m, the Fourier transform $\tilde{t}_\perp(\mathbf{k})$ can become comparable to m in a region of the Brillouin zone, i.e., we may have a situation where

$$t_\perp \ll T \ll \tilde{t}(\mathbf{0}) \approx m. \tag{3}$$

In this case an interesting "hybrid" state combining 1D features with 3D features develops. In particular, the low-energy sector corresponds to a 3D metal with a small Fermi surface and quasiparticles interacting with well-developed collective modes. The existence of the regime (3) is ensured by making the interchain tunneling long ranged.

The dimensional crossover from a quasi-one-dimensional Mott insulator to an anisotropic 3D Fermi liquid, as a function of the strength $t_\perp$ of the interchain hopping, is sketched in Fig. 1.

The purpose of the present work is to derive an effective theory for the low-energy degrees of freedom in the "1D Mott insulator/3D Fermi liquid hybrid" regime and to analyze its instabilities towards 3D order at sufficiently low temperatures.

II. THE MODEL

The model we study is the Hubbard model with a strongly anisotropic hopping,

$$H = -t\sum_{n,\mathbf{l},\sigma}[c^\dagger_{n,\mathbf{l},\sigma}c_{n+1,\mathbf{l},\sigma} + \text{H.c.}] + U\sum_{n,\mathbf{l}} n_{j,\mathbf{l},\uparrow}n_{j,\mathbf{l},\downarrow} + \sum_{\mathbf{l},\mathbf{m},n,p,\sigma} t^{np}_{\mathbf{lm}}c^\dagger_{n,\mathbf{l},\sigma}c_{p,\mathbf{m},\sigma}. \tag{4}$$

For definiteness we consider the chain direction to be z, so that $\mathbf{l}=(l_x,l_y)$, $\mathbf{m}=(m_x,m_y)$ label Hubbard chains, and n, p label the sites along a given chain.

As we have mentioned before, the hopping integrals in the transverse directions are supposed to be small in comparison to t. In the limit $t_\perp=0$ and at half filling the model has a Mott-Hubbard gap m. We work in a regime where the magnitude of this gap is much smaller than the bandwidth $W \approx 4t$. In our previous paper[3] the transverse hopping was treated in a random phase approximation (RPA). In order to suppress corrections to the RPA (at least in some temperature intervals) we assume that the transverse hopping is long ranged (see below).

A. Uncoupled, Mott-insulating chains

Let us briefly discuss the low-energy physics for uncoupled chains. In order to ease notations we suppress the chain index ($\mathbf{l}$). Keeping only the low-energy modes around the two Fermi points $\pm k_F$, the electron annihilation operators are decomposed as

$$c_{n,\sigma} = \sqrt{a_0}[\exp(ik_Fx)R_\sigma(x) + \exp(-ik_Fx)L_\sigma(x)], \tag{5}$$

where a_0 is the lattice spacing, $x=ja_0$, and $k_F=\pi/2a_0$. The fermionic creation operators for left and right moving Fermions are bosonized, using the following conventions:

$$L^\dagger_\sigma(x) = \frac{\eta_\sigma}{\sqrt{2\pi}}e^{if_\sigma\pi/4}\exp\left(-\frac{i}{2}\overline{\phi}_c\right)\exp\left(-\frac{if_\sigma}{2}\overline{\phi}_s\right),$$

$$R^\dagger_\sigma(x) = \frac{\eta_\sigma}{\sqrt{2\pi}}e^{if_\sigma\pi/4}\exp\left(\frac{i}{2}\phi_c\right)\exp\left(\frac{if_\sigma}{2}\phi_s\right), \tag{6}$$

where η_a are the Klein factors with $\{\eta_a,\eta_b\}=2\delta_{ab}$ and where $f_\uparrow=1$, $f_\downarrow=-1$. The chiral boson fields ϕ_a and $\overline{\phi}_a$ fulfill the following commutation relations:

$$[\phi_a(x),\overline{\phi}_a(y)] = 2\pi i, \quad a=c,s. \tag{7}$$

In terms of the chiral fields ϕ_a and $\overline{\phi}_a$ we define the canonical Bose fields Φ_a and their dual fields Θ_a by

$$\Phi_a = \phi_a + \overline{\phi}_a, \quad \Theta_a = \phi_a - \overline{\phi}_a. \tag{8}$$

The low-energy effective Hamiltonian density for a single chain takes the following bosonic form:

$$\mathcal{H}_s = \frac{v_s}{16\pi}[(\partial_x\Theta_s)^2 + (\partial_x\Phi_s)^2] - g\mathbf{J}\cdot\overline{\mathbf{J}},$$

$$\mathcal{H}_c = \frac{v_c}{16\pi}[(\partial_x\Theta_c)^2 + (\partial_x\Phi_c)^2] + g\mathbf{I}\cdot\overline{\mathbf{I}}. \tag{9}$$

Here I^α and $\overline{I^\alpha}$ (J^α and $\overline{J^\alpha}$) are the chiral components of the $SU(2)$ pseudospin (spin) currents,

$$I^z = -\frac{1}{4\pi}\partial_x\phi_c, \quad I^+ = \frac{\eta_\uparrow\eta_\downarrow}{2\pi}e^{i\phi_c},$$

$$J^z = -\frac{1}{4\pi}\partial_x\phi_s, \quad J^+ = i\frac{\eta_\uparrow\eta_\downarrow}{2\pi}e^{i\phi_s}. \tag{10}$$

The current-current interaction in the spin sector of (9) is marginally irrelevant, and we will ignore it in what follows. We note that doing so enhances the symmetry in the spin sector from $SU(2)$ (spin rotational symmetry) to $SU(2)$

$\times SU(2)$ (rotational symmetry of the left and right sectors).

1. Single-particle Green's function

The single-particle Green's function for the half-filled Hubbard model was obtained in the framework of the form-factor approach in Refs. 3 and 11. In particular, when the charge and spin velocities are equal we have

$$G_0(\omega, \pm k_F + q) = \frac{Z_0}{i\omega \mp vq}\left[1 - \frac{m}{\sqrt{m^2 + \omega^2 + (vq)^2}}\right], \tag{11}$$

where $Z_0 \approx 0.921\,862$. In order to obtain the above expression for G_0 we took into account only processes involving the emission of a single, massive holon and a cascade of gapless spinons.

2. Spin sector

The spin operators $S_n^\alpha = \frac{1}{2} c_{n,a}^\dagger \sigma_{ab}^\alpha c_{n,b}$ are expressed in terms of the left and right moving Fermi fields by

$$\begin{aligned} S_j^\alpha &\simeq (-1)^j \frac{a_0}{2}[R_a^\dagger(x)\sigma_{ab}^\alpha L_b(x) + \text{H.c.}] \\ &\quad + \frac{a_0}{2}[R_a^\dagger(x)\sigma_{ab}^\alpha R_b(x) + R \to L] \\ &\equiv a_0[(-1)^j n^\alpha(x) + J^\alpha(x)]. \end{aligned} \tag{12}$$

The bosonized expressions for the staggered components of the spin operators are

$$R_a^\dagger(x)\sigma_{ab}^\alpha L_b(x) \simeq \frac{1}{\pi i\sqrt{2a_0}} \exp\left(\frac{i}{2}\Phi_c\right) \mathrm{tr}(g\sigma^\alpha), \tag{13}$$

where we have replaced the product of the Klein factors by their expectation values,

$$\langle \eta_\uparrow \eta_\downarrow \rangle = -i, \tag{14}$$

and where the matrix field g is expressed in terms of the spin boson Φ_s and its dual field Θ_s by

$$g = \sqrt{\frac{a_0}{2}} \begin{pmatrix} \exp\left(\frac{i}{2}\Phi_s\right) & i\exp\left(-\frac{i}{2}\Theta_s\right) \\ i\exp\left(\frac{i}{2}\Theta_s\right) & \exp\left(-\frac{i}{2}\Phi_s\right) \end{pmatrix}. \tag{15}$$

At $T=0$ we have

$$\langle g_{\alpha\beta}(\tau,x) g_{\gamma\delta}^\dagger(0,0)\rangle = \delta_{\alpha\delta}\delta_{\beta\gamma} \frac{a_0}{2\sqrt{v^2\tau^2 + x^2}}. \tag{16}$$

Using (15) one can easily calculate the multipoint correlation functions of g.

The action (9) describing the collective spin excitations on each chain is equivalent to the $SU_1(2)$ Wess-Zumino-Novikov-Witten (WZNW) model once we drop the marginally irrelevant interaction of spin currents. The WZWN action for the matrix field $g(\tau,x)$ is given by

$$\begin{aligned} W[g] &= \frac{1}{16\pi}\int d^2x\, \mathrm{Tr}[\partial^\mu g^\dagger \partial_\mu g] \\ &\quad + -i\frac{\epsilon_{\mu\nu\lambda}}{24\pi}\int_B d^3x\, \mathrm{Tr}[g^\dagger\partial^\mu g g^\dagger \partial^\nu g g^\dagger \partial^\lambda g], \end{aligned} \tag{17}$$

where $x_1 = v\tau$, $x_2 = x$, $\partial_\mu = \partial/\partial x^\mu$, B is a three-dimensional half space ($x_3 \leqslant 0$) whose boundary at $x_3 = 0$ coincides with the two-dimensional $(v\tau, x)$ plane, and g is an arbitrary extrapolation of the function defined on the two-dimensional space $x_3 = 0$, which approaches 1 at $x_3 \to -\infty$. The action (17) is invariant under $SU(2) \times SU(2)$ transformations $g \to U g \tilde{U}^\dagger$. The marginally irrelevant interactions of spin currents breaks this symmetry down to the diagonal spin-rotational $SU(2)$ $g \to U g U^\dagger$. The form (17) of the action for the spin degrees of freedom is significantly more complicated than the free boson representation (9). The latter is very convenient for calculations in one dimension, but may be less useful when one considers interchain coupling due to the fact that the dual field Θ_s is nonlocal with respect to Φ_s. The formulation in terms of the matrix field g has the advantage of the fundamental field being the order parameter itself. In fact, $W[g]$ is the Ginzburg-Landau action for a 1D spin-$\frac{1}{2}$ antiferromagnet.

3. Three-point function

Some important ingredients in our analysis are the three-point functions of the form $\langle \mathrm{Tr}[g(\mathbf{z})\sigma^\alpha] R_a^\dagger(\mathbf{z_1}) L_b(\mathbf{z_2})\rangle$. The large-distance asymptotics of these correlators can be evaluated by using the results of[11]

$$\begin{aligned} \langle \mathrm{Tr}[g(\mathbf{z})\sigma^+] R_\downarrow^\dagger(\mathbf{z_1}) L_\uparrow(\mathbf{z_2})\rangle &= -i\frac{\langle \eta_\downarrow \eta_\uparrow\rangle}{2\pi}\langle \mathrm{Tr}[g(\mathbf{z})\sigma^+] e^{-(i/2)\phi_s(\mathbf{z_1})} e^{(i/2)\bar{\phi}_s(\mathbf{z_2})}\rangle_s \langle e^{(i/2)\phi_c(\mathbf{z_1})} e^{(i/2)\bar{\phi}_c(\mathbf{z_2})}\rangle_c \\ &\simeq i\frac{\langle \eta_\downarrow \eta_\uparrow\rangle}{2\pi}\langle \mathrm{Tr}[g(\mathbf{z})\sigma^+] e^{-(i/2)\phi_s(\mathbf{z_1})} e^{(i/2)\bar{\phi}_s(\mathbf{z_2})}\rangle_s \frac{Z_1\sqrt{a_0}}{\pi} e^{3i\pi/4} K_0(m r_{12}) \\ &\simeq \hat{Z}\langle \eta_\downarrow \eta_\uparrow\rangle K_0(m r_{12}) \langle \mathrm{Tr}[g(\mathbf{z})\sigma^+]\mathrm{Tr}[g(\mathbf{z}_+)\sigma^-]\rangle_s, \end{aligned} \tag{18}$$

where $\mathbf{z}_{1,2}=(\tau_{1,2},x_{1,2})$, $r_{12}=|\mathbf{z}_1-\mathbf{z}_2|$ and $\mathbf{z}_+=[(\tau_1+\tau_2)/2,(x_1+x_2)/2]$. The constant $\hat{Z}$ is related to the normalization Z_0 of the single-particle Green's function by[11]

$$\hat{Z}=-\frac{Z_0}{\pi^{3/2}}\sqrt{\frac{m}{va_0}}. \tag{19}$$

The calculation we have just carried out can be summarized by the following approximate relations,

$$R_a^\dagger(\mathbf{z_1})\sigma_{ab}^\alpha L_b(\mathbf{z_2})\to i\hat{Z}K_0(mr_{12})\mathrm{Tr}[g(\mathbf{z}_+)\sigma^\alpha],$$

$$L_a^\dagger(\mathbf{z_1})\sigma_{ab}^\alpha R_b(\mathbf{z_2})\to i\hat{Z}K_0(mr_{12})\mathrm{Tr}[g(\mathbf{z}_+)\sigma^\alpha]. \tag{20}$$

The approximation (20) fails at small distances. In order to remove the logarithmic singularity of K_0 one needs to include terms corresponding to the multiple production of solitons and antisolitons. At energies much smaller than the Mott gap, the fusion (20) gives rise to the spin-fermion vertex depicted in Fig. 2.

B. Long-range interchain hopping

In order to have a small parameter in our theory we consider the interchain hopping to be long ranged, such that the Fourier transform of the hopping matrix elements strongly depends on the wave vector. This is a well-known trick (see, for example, Ref. 12) and results in a controlled "loop" expansion, where every integration over the transverse momenta leads to a small factor κ_0^2 in three dimensions, where κ_0 is the inverse range of the interchain tunneling. The interchain hopping may be taken long ranged both along and perpendicular to the chain direction. In order to simplify the calculations, we will constrain our discussion to the case where $t_{\mathbf{lm}}^{np}=t(\mathbf{l}-\mathbf{m})\delta_{n,p}$, i.e., the interchain hopping has no component along the chain direction and depends only on the distance between chains. The Fourier transform of the interchain tunneling is then given by

$$\tilde{t}_\perp(\mathbf{k}_\perp)=\sum_{\mathbf{m}} t_{\mathbf{lm}}\exp[i\mathbf{k}_\perp\cdot(\mathbf{l}-\mathbf{m})a_\perp]. \tag{21}$$

In the following we choose the interchain hopping such that it respects the particle-hole symmetry:

$$c_{n,\mathbf{l},\sigma}\leftrightarrow(-1)^{n+l_x+l_y}c_{n,\mathbf{l},\sigma}^\dagger, \tag{22}$$

which implies that

$$\tilde{t}_\perp(\mathbf{k}_\perp+\mathbf{Q})=-\tilde{t}_\perp(\mathbf{k}_\perp), \tag{23}$$

where

$$\mathbf{Q}=\left(\frac{\pi}{a_\perp},\frac{\pi}{a_\perp}\right), \tag{24}$$

is the antiferromagnetic wave vector in the direction transverse to the chains. It is straightforward to generalize our following analysis to non-particle-hole symmetric cases. The basic assumptions underlying our model are then summarized in the following inequalities:

FIG. 2. The fermion-spinon interaction generated by fusion (20).

$$W\gg m\sim|\tilde{t}_\perp(\mathbf{0})|=|\tilde{t}_\perp(\mathbf{Q})|\gg\tilde{t}_\perp(\mathbf{p}_\perp). \tag{25}$$

Here $W=4t$ and m are the bandwidth and Mott gap for uncoupled chains, respectively, and $|\mathbf{p}_\perp a_\perp|,|(\mathbf{p}_\perp-\mathbf{Q})a_\perp|\gg\kappa_0$. The small parameter κ_0 characterizes the support of $\tilde{t}_\perp(\mathbf{k}_\perp)$ in momentum space. The precise form of the momentum dependence of $\tilde{t}_\perp$ is supposedly unimportant, but in order to simplify the concrete calculations we shall use the following model:

$$\tilde{t}_\perp(\mathbf{k}_\perp)=-\frac{t_0}{1+|\mathbf{k}_\perp a_\perp|^2\kappa_0^{-2}},\quad |\mathbf{k}_\perp a_\perp|\ll 1. \tag{26}$$

Within the model (26) the integration over the transverse wave vectors may be replaced by integration over $t\equiv t_\perp(\mathbf{k}_\perp)$,

$$a_\perp^2\int\frac{d^2k_\perp}{4\pi^2}f(t)\approx\frac{\kappa_0^2t_0}{4\pi}\int_{\kappa_0^2t_0/4\pi^2}^{t_0}\frac{dt}{t^2}[f(t)+f(-t)]. \tag{27}$$

Some readers may find that our approach is similar to dynamical mean field theory in an *infinitely dimensional* space. This is not the case; the difference comes from the fact that in our model the transverse density of states is constant on the zone boundary. This feature strengthens the influence of fermionic coherent modes and utterly changes the physics (see the discussion in Sec. VII).

III. PERTURBATION THEORY IN THE INTERCHAIN TUNNELING

As we have already mentioned, the perturbation theory in the interchain tunneling can be reorganized in terms of a loop expansion. Every integration over the transverse momenta generates a small factor κ_0^2. We will refer to the leading order $\mathcal{O}(\kappa_0^0)$ in this expansion as random phase approximation (RPA).

The RPA expression for the single-particle Green's function G was derived in Ref. 3 and is given by

$$G(\omega,\pm k_F+q,\mathbf{k}_\perp)=\frac{G_0(\omega,\pm k_F+q)}{1-\tilde{t}_\perp(\mathbf{k}_\perp)G_0(\omega,\pm k_F+q)}. \tag{28}$$

Here G_0 is the single-particle Green's function for an individual chain (11). In a purely one-dimensional Mott insulator the electron is a composite particle, and, as a result, the spectral function is incoherent. Coherent electronic excitations reappear as soon as the interchain tunneling is turned on. They can be understood as antiholon-spinon bound states, and they occur at energies *below* the Mott gap. When $t_\perp$ exceeds a certain critical value, the dispersion of the coherent mode crosses the chemical potential, and a Fermi surface is formed. As a consequence of particle-hole symmetry, at half-filling this Fermi surface consists of electronlike and holelike

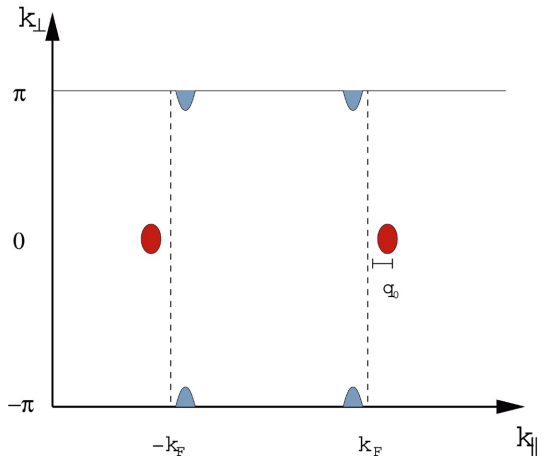

FIG. 3. (Color) The Brillouin zone with the electron (red ovals) and holelike (blue semiovals) Fermi pockets of a two-dimensional lattice. The noninteracting Fermi surface is shown as a dashed line.

pockets of equal volume. A sketch of such a Fermi surface is shown in Fig. 3. A convenient measure for the strength of the interchain coupling is given by the quantity,

$$\mathcal{Z} \equiv \frac{Z_0 t_0}{m}, \tag{29}$$

where t_0 is defined in (26). The RPA form (28) for the Green's function features a pole corresponding to a coherent quasiparticle mode. This mode crosses the chemical potential when $\mathcal{Z}$ exceeds the critical value,

$$\mathcal{Z}_c = 3.330\,19\ldots, \tag{30}$$

and a Fermi surface is present for all $\mathcal{Z} > \mathcal{Z}_c$.

Having in hand the expression for the chain single-particle Green's function, we may use it to define a dressed interchain hopping $\tilde{T}_{R,L}(\omega, q, \mathbf{k}_\perp)$ by summing the diagrams shown in Fig. 4. This results in

$$T_{R,L}(\omega, q, \mathbf{k}_\perp) = \frac{\tilde{t}_\perp(\mathbf{k}_\perp)}{1 - \tilde{t}(\mathbf{k}_\perp) G_0(\omega, \pm k_F + q)}, \tag{31}$$

where the $+$ sign corresponds to R and the $-$ sign to L, respectively. We note that the dressed interchain hopping is equal to the propagator of the Hubbard-Stratonovich field that can be introduced to decouple the interchain hopping.[13]

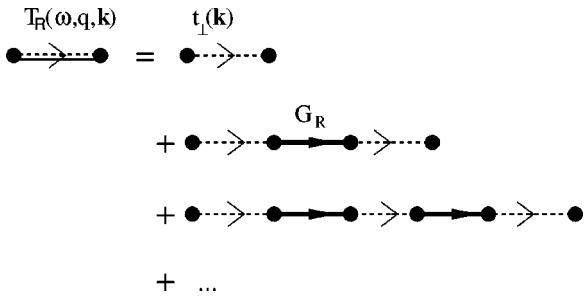

FIG. 4. The dressed interchain hopping.

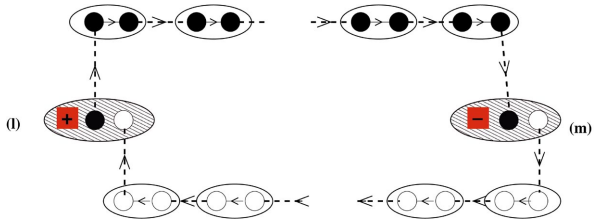

FIG. 5. (Color) Real-space diagrams that contribute to the two-point function of staggered magnetizations between chains (l) and (m).

A. The spin sector in RPA

In the RPA, the spin sector remains one-dimensional and critical. This can be seen as follows. Let us consider the real-space correlator between the staggered components of spins on different chains **l** and **m**,

$$\langle n^+_{j,\mathbf{l}}(t) n^-_{1,\mathbf{m}}(0) \rangle. \tag{32}$$

Within perturbation theory in the interchain hopping, we need at least one right-moving and left-moving fermion operator each on chains l and m in order to obtain a nonzero expectation value in the spin sector. The only ways to achieve this are shown in Fig. 5. Here the dashed lines denote the bare interchain hopping, the ellipses enclosing two black (white) circles represent the purely 1D Green's function of right-moving (left moving) electrons on a given chain, and the ellipses enclosing two circles and a hexagon stand for the three-point function (18). Clearly all such diagrams involve at least one integration over the transverse momentum. Hence, within the RPA, the spin-spin correlation functions remain entirely one-dimensional and spins on different chains remain uncorrelated.

B. Excitation spectrum in RPA

From the discussion above it is clear that for sufficiently strong interchain hopping $\mathcal{Z} > \mathcal{Z}_c$ the RPA leads to two types of gapless excitations:

(i) fermionic particle and hole excitations over the Fermi surface with anisotropic 3D dispersions.

(ii) collective excitations of the spin degrees of freedom. These are of a purely 1D nature and do not have a dispersion in the direction transverse to the chains.

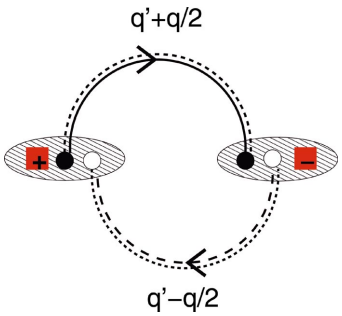

FIG. 6. (Color) Leading-order $\mathcal{O}(\kappa_0^2)$ contribution to the interchain exchange.

If one goes beyond the RPA, the interactions between these two types of excitations will be generated. In the following we determine the form of these interactions and study their effects. To go beyond the RPA in principle requires knowledge of the two-particle Green's function of uncoupled Mott-insulating chains. However, if one restricts one's attention to the regime of energies that are small compared to the Mott gap, the three-point function (18) (which corresponds to a particular limit of the two-particle Green's function) suffices.

IV. INTERCHAIN EXCHANGE AND ESTIMATE OF THE TRANSITION TEMPERATURE

Although it is obvious that corrections to RPA are of higher order in the small parameter κ_0, they will diverge at small temperatures. Therefore RPA works only at finite temperatures, and for its consistency the transition temperature (below which the system is three-dimensionally ordered) must be much smaller than the Mott-Hubbard gap m. It is therefore important to estimate the corresponding corrections to RPA and their temperature dependence. As the first step in taking into account corrections to RPA we have to estimate the interchain Ruderman-Kittel-Kasuya-Yosida (RKKY) interaction. As we have shown in Sec. II A 3, there is a three-point "vertex" that couples the spin degrees of freedom to the fermionic quasiparticles. In the second-order perturbation theory in this interaction, an interchain exchange interaction between the spin degrees of freedom is generated. The corresponding action is given by

$$S_{\mathrm{xc}} = \int \prod_{j=1}^{2} d\tau_j dx_j \sum_{\mathbf{l}\neq\mathbf{m}} J_{\mathbf{lm}}(x_1 - x_2, \tau_1 - \tau_2) \times \mathrm{Tr}[\mathbf{g}_{\mathbf{l}}(\tau_1, \mathbf{x}_1)\mathbf{g}^{\dagger}_{\mathbf{m}}(\tau_2, \mathbf{x}_2)]. \tag{33}$$

The Fourier transform of the leading-order (in κ_0) exchange matrix element is given by the "bubble" diagram shown in Fig. 6, where the doubles lines are the dressed interchain hoppings for left-moving and right-moving fermions and the squares denote the elements of the matrix field. The result is

$$\tilde{J}(\omega, q, \mathbf{q}_\perp) = \hat{Z}^2 \int \frac{d\omega' dq'}{(2\pi)^2} a_\perp^2 \int d^2k_\perp \left[\frac{v}{m^2 + \omega'^2 + (vq')^2}\right]^2 T_R\left(\omega' + \frac{\omega}{2}, q' + \frac{q}{2}, \mathbf{k}_\perp\right) \times T_L\left(\omega' - \frac{\omega}{2}, q' - \frac{q}{2}, \mathbf{q}_\perp - \mathbf{k}_\perp\right). \tag{34}$$

To make the calculations easier, we use the k dependence (26) so that the sum over the transverse wave vectors is replaced by integration over t according to (27). Since $\tilde{t}(\mathbf{k}_\perp)$ is peaked near zero and $\mathbf{Q}$, there are two interesting wave vectors: $\mathbf{q}_\perp = 0$ and $\mathbf{q}_\perp = \mathbf{Q}$.

A. Case 1: $\mathcal{Z} < \mathcal{Z}_c$

In this case the coherent electron modes still have a gap and no Fermi surface is formed in the RPA. Using (27) to carry out the summation over the transverse momenta we obtain

$$\tilde{J}(0,0,\mathbf{0}) \approx \mathcal{C}_1 \int_0^\infty ds s \frac{\arctan[\mathcal{Z}G(s)]}{(1+s^2)^2 G(s)} \equiv \alpha_0 \mathcal{C}_1, \tag{35}$$

where $\mathcal{Z} = Z_0 t_0 / m$ is defined in (29) and

$$\mathcal{C}_1 = \hat{Z}^2 \kappa_0^2 t_0 \frac{v}{m Z_0} = \frac{\mathcal{Z}\kappa_0^2}{\pi^3 a_0} m, \tag{36}$$

and

$$G(s) = s^{-1}\left[1 - \frac{1}{\sqrt{s^2+1}}\right]. \tag{37}$$

As expected, this interaction is of the order of $\kappa_0^2 t_0$. The numerical factor α_0 ranges between 0 for $\mathcal{Z} = 0$ and 2.81 for $\mathcal{Z} \to 3.33\,019$. The exchange at momentum transfer $\mathbf{Q}$ is

$$\tilde{J}(0,0,\mathbf{Q}) \approx -\frac{\mathcal{C}_1}{2} \int_0^\infty ds s \frac{\ln\left[\frac{1+\mathcal{Z}G(s)}{1-\mathcal{Z}G(s)}\right]}{(1+s^2)^2 G(s)} = -\alpha_Q \mathcal{C}_1, \tag{38}$$

where α_Q varies between 0 for $\mathcal{Z} = 0$ and 3.07 for $\mathcal{Z} \to \mathcal{Z}_c$.

B. Case 2: $\mathcal{Z} > \mathcal{Z}_c$

In this case a Fermi surface in the form of electron and hole pockets is present. The presence of zero-energy modes does not really affect the exchange at zero-momentum transfer, which is given by

$$\tilde{J}(0,0,\mathbf{0}) \approx \mathcal{C}_1 \int_0^\infty ds \frac{s f(s)}{(1+s^2)^2 G(s)} = \alpha_0' \mathcal{C}_1, \tag{39}$$

where

$$f(s) = 2\arctan[\xi(s)\mathcal{Z}G(s)] - \arctan[\mathcal{Z}G(s)],$$

$$\xi(s) = \min(1, [\mathcal{Z}G(s)]^{-1}). \tag{40}$$

We find that α_0' starts at 1.405 for $\mathcal{Z} \to 3.33\,019$, then goes through a maximum of approximately 1.48 around $\mathcal{Z}$

≈ 4.18, and then diminishes slowly. Hence the exchange at wave number zero plays a subdominant role.

Let us now turn to the exchange at wave number $\mathbf{Q}$. We find that there is a logarithmic divergence in (34), which is related to the Fermi-surface formation and will be discussed later in more detail. We regularize the divergence by temperature. This may be done by replacing the ω'-integral in (34) by a sum over Matsubara frequencies and substituting the finite-temperature Green's function for their $T=0$ analogs in the dressed interchain hoppings $\tilde{T}_{R,L}$ in (34). At low temperatures the single-particle Green's function is given by[8]

$$G_R(\omega_n,q)=\int_{-\infty}^{\infty}dx\frac{A_R(x,q)}{i\omega_n-x},$$

$$A_R(\omega,q)=\frac{Z_0}{4\pi^2 m}\sqrt{\frac{2m}{T}}\left[\frac{m}{|\omega-vq|}\right]^{3/2}\times\mathrm{Re}\left[\sqrt{-2i}B\left(\frac{1}{4}-\frac{i}{2}\frac{\omega^2-v^2q^2-m^2}{2\pi T|\omega-vq|},\frac{1}{2}\right)\right]. \quad (41)$$

The singular piece of $\tilde{J}^{\mathrm{sing}}(0,0,\mathbf{Q})$ diverges logarithmically with temperature and is estimated as

$$\tilde{J}^{\mathrm{sing}}(0,0,\mathbf{Q})\approx -\mathcal{C}_1\ln\left[\frac{m}{T}\right]\int_{s_-}^{s_+}ds\frac{s[G(s)]^{-1}}{(1+s^2)^2}, \quad (42)$$

where $s_\pm$ are solutions to the equation,

$$1-\mathcal{Z}G(s_\pm)=0. \quad (43)$$

In order to establish the exchange at nonzero values of ω and q we have calculated $\tilde{J}(\omega,q,\mathbf{Q})$ numerically at small temperatures. Rather than using the finite-T Green's function (41) we work with the $T=0$ expression (11) and replace ω by the discrete Matsubara frequencies. For small temperatures this is a reasonable approximation. We find that $|\tilde{J}(\omega,q,\mathbf{Q})|$ is largest at $\omega=0=q$.

In addition to the singular piece (42) there also is a regular contribution to the exchange. As long as we are close to the transition, i.e.,

$$\frac{\mathcal{Z}-\mathcal{Z}_c}{\mathcal{Z}_c}\ll 1, \quad (44)$$

we may estimate the regular contribution to the exchange by its value at the critical strength $\mathcal{Z}_c$ of the interchain tunneling. The latter is given by (38)

$$\tilde{J}^{\mathrm{reg}}(0,0,\mathbf{Q})\approx -3.071\mathcal{C}_1. \quad (45)$$

In the regime (44),

$$\tilde{J}^{\mathrm{sing}}(0,0,\mathbf{Q})\approx -1.318\sqrt{\mathcal{Z}-\mathcal{Z}_c}\mathcal{C}_1\ln\left[\frac{m}{T}\right]. \quad (46)$$

The total exchange constant at wave number $\mathbf{Q}$ is then estimated as

$$\tilde{J}(0,0,\mathbf{Q})\approx -\mathcal{C}_1\left(3.071+1.318\sqrt{\mathcal{Z}-\mathcal{Z}_c}\ln\left[\frac{m}{T}\right]\right). \quad (47)$$

Having determined the exchange constant, we are now in a position to estimate the temperature at which a magnetic instability develops. In the absence of interchain hopping the correlation functions of the matrix field at $T=0$ are given by (16). At $T>0$ we have

$$\langle g_{\alpha\beta}(\tau,x)g^{+}_{\gamma\delta}(0,0)\rangle=\delta_{\alpha\delta}\delta_{\beta\gamma}\frac{\pi Ta_0/v}{2\left|\sinh\left(\frac{\pi T}{v}[x+iv\tau]\right)\right|}, \quad (48)$$

if we neglect the marginally irrelevant current-current interaction in the spin-sector of Hamiltonian (9), describing the 1D Mott insulating chains. If one takes it into account in renormalization-group-improved perturbation theory one obtains[14]

$$\langle \mathrm{tr}(g\sigma^\alpha)\mathrm{tr}(g^\dagger\sigma^\beta)\rangle=\delta_{\alpha\beta}\frac{\sqrt{\ln\left[\frac{\Lambda}{T}\right]}\pi Ta_0v^{-1}}{\left|\sinh\left(\frac{\pi T}{v}[x+iv\tau]\right)\right|}, \quad (49)$$

where Λ is a high-energy cutoff, which we may take to be of the order of the hopping integral along the chain direction. Carrying out an analogous calculation for the dimerization operator we find

$$\langle \mathrm{tr}(g)\mathrm{tr}(g^\dagger)\rangle=\delta_{\alpha\beta}\frac{\left(\ln\left[\frac{\Lambda}{T}\right]\right)^{-3/2}\pi Ta_0v^{-1}}{\left|\sinh\left(\frac{\pi T}{v}[x+iv\tau]\right)\right|}. \quad (50)$$

Upon Fourier transformation and analytical continuation one finds the following result for the dynamical magnetic susceptibility of the uncoupled chain system:[15]

$$\chi_{1\mathrm{d}}(\omega,q)=-\frac{a_0\sqrt{\ln\left[\frac{\Lambda}{T}\right]}}{2T}\frac{\Gamma\left[\frac{1}{4}-i\frac{\omega-vq}{4\pi T}\right]\Gamma\left[\frac{1}{4}-i\frac{\omega+vq}{4\pi T}\right]}{\Gamma\left[\frac{3}{4}-i\frac{\omega-vq}{4\pi T}\right]\Gamma\left[\frac{3}{4}-i\frac{\omega+vq}{4\pi T}\right]}. \quad (51)$$

The dimerization susceptibility is equal to (51) apart from the prefactor, in which $\sqrt{\ln[\Lambda/T]}$ is replaced by $(\ln[\Lambda/T])^{-3/2}$. Hence the staggered spin susceptibility is always more singular than the dimerization susceptibility, and as a result the dominant instability of the spin sector is towards the Néel order. The enhancement of the spin susceptibility as compared to the dimerization susceptibility is caused by the leading irrelevant operator in the Hamiltonian, namely the interaction of the spin currents. If we were to add an interaction to the underlying lattice Hamiltonian in order to eliminate this interaction, the symmetry between the dimerization and the staggered components of the spins

would be broken by some other irrelevant operator. The dynamical susceptibility of the coupled chains system can be determined by an expansion in the interchain coupling of the type discussed in Refs. 16 and 17. The leading term is given by the random phase approximation,

$$\chi_{3d}(\omega,q,\mathbf{p}_\perp)=\frac{\chi_{1d}(\omega,q)}{1-2\tilde{J}(\omega,q,\mathbf{p}_\perp)\chi_{1d}(\omega,q)}. \tag{52}$$

Given the expression (52) for the dynamical susceptibility, we may obtain an estimate for the transition temperature T_c, below which the three-dimensional magnetic-long-range order develops. T_c is defined as the temperature at which a zero frequency pole develops in χ_{3d}. Given that $\chi_{1d}(0,q)$ is peaked at $q=0$ and $\tilde{J}$ is peaked at $q=0$ and $\mathbf{p}=\mathbf{Q}$, we obtain the following condition-fixing T_c:

$$1-2\tilde{J}(0,0,\mathbf{Q})\chi_{1d}(0,0)=0. \tag{53}$$

Replacing $\tilde{J}(0,0,\mathbf{Q})$ by (47) we arrive at the following equation determining the transition temperature T_c:

$$\frac{T_c}{m}\approx 2.887\kappa_0^2\sqrt{\ln\left[\frac{\Lambda}{T_c}\right]}\times\left(1+0.429\sqrt{\mathcal{Z}-\mathcal{Z}_c}\ln\left[\frac{m}{T_c}\right]\right). \tag{54}$$

Let us consider the two limiting cases in which either the regular (45) or the singular part (46) of the exchange dominates and drives the transition. The first case occurs if we are very close to the point where the Fermi pockets are first formed and $\mathcal{Z}-\mathcal{Z}_c\ll[\ln(\kappa_0^2)]^{-2}$. Then the transition temperature is roughly equal to

$$\frac{T_c}{m}\approx 2.887\kappa_0^2\sqrt{\ln\left[\frac{\Lambda}{m\kappa_0^2}\right]}. \tag{55}$$

The second case occurs if $\mathcal{Z}-\mathcal{Z}_c\gg[\ln(\kappa_0^2)]^{-2}$ and then,

$$\frac{T_c}{m}\approx 1.239\kappa_0^2\delta\sqrt{\ln\left[\frac{\Lambda}{m\kappa_0^2\delta}\right]}\ln\left[\frac{1}{\kappa_0^2\delta}\right], \tag{56}$$

where $\delta=\sqrt{\mathcal{Z}-\mathcal{Z}_c}$.

V. EFFECTIVE THEORY AT LOW ENERGIES; THE RESIDUAL INTERACTIONS

Now we are in the position of writing the low-energy effective action for the metallic state. This effective action describes the interactions of the low-energy modes, i.e., the coherent fermions and the order-parameter field g_{ab}. In Sec. IV we calculated the interchain coupling for the g field. It contains a part coming from states far from the chemical potential and a part with logarithmic divergences coming from the states close to the Fermi surface. We can isolate the first piece and include it into the effective action of g,

$$S_{sp}=\sum_{\mathbf{n}}W[g_{\mathbf{n}}]+\sum_{\mathbf{m},\mathbf{l}}J_{\mathbf{ml}}\int d\tau dx\,\mathrm{Tr}[\mathrm{g}_{\mathbf{m}}(\tau,\mathrm{x})\mathrm{g}^{\dagger}_{\mathbf{l}}(\tau,\mathrm{x})], \tag{57}$$

where to first approximation,

$$J_{\mathbf{nl}}\approx\frac{Z_0^2}{\pi^2 m a_0}t_{\mathbf{nl}}^2. \tag{58}$$

This part of the action plays the role of the sigma model in the spin-fermion model by Chubukov, Pines, and Schmalian (see Ref. 2 and references therein). Taken in isolation, this model has an instability at some temperature T_c that can be estimated from the RPA expression for the dynamical magnetic susceptibility in complete analogy with our calculation in Sec. IV B. Since the coherent fermions are low-energy excitations, they cannot be simply integrated out, but their interaction with the g field should be added to the action. The Fermi surface of the coherent fermions is determined by the equation,

$$G_0(0,q)\tilde{t}_\perp(\mathbf{k}_\perp)=1, \tag{59}$$

and it consists of four pockets (two electronlike ones and two holelike ones) as is shown in Fig. 3. Let us consider the situation where the scale of the interchain hopping t_0 is very slightly larger than the minimal value $\bar{t}_0$ required for the formation of a Fermi surface,

$$t_0=\bar{t}_0+\delta t=\sqrt{\frac{11+5\sqrt{5}}{2}}\frac{m}{Z_0}+\delta t. \tag{60}$$

The electron and hole pockets are then shallow and anisotropic, and the Fermi surface is determined by the equation,

$$E(q,\mathbf{k}_\perp)=0, \tag{61}$$

where

$$E(q,\mathbf{k}_\perp)=A_\parallel m\frac{(q-q_0)^2}{q_0^2}+A_\perp m\frac{|\mathbf{k}_\perp a_\perp|^2}{\kappa_0^2}-E_0, \tag{62}$$

$$E_0\approx 0.352\delta t,\quad \frac{vq_0}{m}=\left[\frac{1+\sqrt{5}}{2}\right]^{1/2}\approx 1.27202,$$

$$A_\parallel\approx 0.543,\quad A_\perp\approx 1.27\,202. \tag{63}$$

The electron pockets are formed at $(k_F+q,\mathbf{k}_\perp)$ and $(-k_F-q,\mathbf{k}_\perp)$, whereas the hole pockets are located at $(k_F-q,\mathbf{Q}+\mathbf{k}_\perp)$ and $(-k_F+q,\mathbf{Q}+\mathbf{k}_\perp)$, where q and $\mathbf{k}_\perp$ are determined from (61). Let us denote the annihilation operator of the coherent fermions by $\Psi(\tau,q,\mathbf{k}_\perp)$. The soft modes occur in the vicinity of the electron and hole pockets and it is convenient to decompose $\Psi(\tau,q,\mathbf{k}_\perp)$ accordingly. We denote by $R_e(\tau,q,\mathbf{p}_\perp)$ and $L_e(\tau,q,\mathbf{p}_\perp)$ the annihilation operators in the vicinity of the electron pockets and $(q,\mathbf{p}_\perp)$ is the deviation from $(\pm k_F,0)$. Similarly we denote by $R_h(\tau,q,\mathbf{p}_\perp)$ and $L_h(\tau,q,\mathbf{p}_\perp)$ the annihilation operators in the vicinity of the hole pockets, and $(q,\mathbf{p}_\perp)$ is the deviation from $(\pm k_F,\mathbf{Q})$.

From Eq. (62) we determine that the particle density associated with a single pocket is

$$n\approx 0.027a_\perp^{-2}q_0\kappa_0^2(\mathcal{Z}-\mathcal{Z}_c)^{3/2}. \tag{64}$$

The liquid of quasiparticles becomes degenerate at temperatures of the order of E_0. Comparing them with the transition temperatures [(54) and (56)] we conclude that the degenerate metallic state exists only at

$$\mathcal{Z} - \mathcal{Z}_c \gg \kappa_0^2, \tag{65}$$

corresponding to $na_\perp^2 \gg 0.027 q_0 \kappa_0^5$. Close to the Fermi surface the Green's function (28) can be approximated as

$$G(\omega, \pm k_F + q, \mathbf{k}_\perp) \approx \frac{Z_2}{i\omega - E(\pm q, \mathbf{k}_\perp)}, \tag{66}$$

$$G(\omega, \pm k_F + q, \mathbf{k}_\perp + \mathbf{Q}) \approx \frac{Z_2}{i\omega + E(\mp q, \mathbf{k}_\perp)}, \tag{67}$$

where

$$Z_2 \approx \frac{v q_0}{t_0} \approx 0.352. \tag{68}$$

The expressions (67) exhibit the particle-hole symmetry characteristic of our model at half filling. As usual, we include the residue Z in the coupling constant and replace the fermionic action by the action of the four components of free fermions. The effective action describing the fermions is then given by

$$S_f = a_\perp^2 \int \frac{d\tau d^3\mathbf{k}}{(2\pi)^3} \{R^*_{a,\alpha}(\tau,\mathbf{k})[\partial_\tau - E_a^R(\mathbf{k})]R_{a,\alpha}(\tau,\mathbf{k}) + L^*_{a,\alpha}(\tau,\mathbf{k}) \times [\partial_\tau - E_a^L(\mathbf{k})]L_{a,\alpha}(\tau,\mathbf{k})\}, \tag{69}$$

where $\mathbf{k} = (q, \mathbf{k}_\perp)$, $\alpha = \uparrow, \downarrow$, $a = e, h$, and

$$E_e^{R,L}(\mathbf{k}) = E(\pm q, \mathbf{k}_\perp), \quad E_h^{R,L}(\mathbf{k}) = -E(\mp q, \mathbf{k}_\perp). \tag{70}$$

The fermion-spin vertex is described by the action,

$$S_{\rm int} = a_\perp^4 \int \frac{d\tau d^3\mathbf{k} d^3\mathbf{k}'}{(2\pi)^6} \mathcal{L}_{\rm int}, \tag{71}$$

where

$$\mathcal{L}_{\rm int} = I_{\mathbf{k},\mathbf{k}'} \sum_{a=e,h} R^*_{a,\alpha}(\tau,\mathbf{k}) L_{a,\beta}(\tau,\mathbf{k}') g_{\alpha\beta}(\tau, \mathbf{k} - \mathbf{k}') + I_{\mathbf{k},\mathbf{Q}+\mathbf{k}'} R^*_{e,\alpha}(\tau,\mathbf{k}) L_{h,\beta}(\tau,\mathbf{k}') g_{\alpha\beta}(\tau, \mathbf{k} - \mathbf{Q} - \mathbf{k}') + I_{\mathbf{Q}+\mathbf{k},\mathbf{k}'} R^*_{h,\alpha}(\tau,\mathbf{k}) L_{e,\beta}(\tau,\mathbf{k}') g_{\alpha\beta}(\tau, \mathbf{k} + \mathbf{Q} - \mathbf{k}') + \text{H.c.},$$

$$I_{\mathbf{k},\mathbf{k}'} = 2\pi \frac{v \hat{Z} Z_2}{m^2} \tilde{t}_\perp(\mathbf{k}) \tilde{t}_\perp(\mathbf{k}'). \tag{72}$$

All wave vectors in the above formulas lie close to the noninteracting Fermi surface, and therefore their longitudinal components are small in comparison to π: $|q| \ll \pi a_0$. The entire approach is valid only when the volumes inside of the Fermi surfaces are small. One then can neglect the momentum dependence of the exchange constant in Eq. (72). The sign of the exchange constant depends on the "pocket index" a, b,

$$I_{ab} \approx \gamma m \begin{pmatrix} 1 & -1 \\ -1 & 1 \end{pmatrix}, \tag{73}$$

where γ is a constant. The interaction can be cast in the form

$$\mathcal{L}_{\rm int} = \gamma m \Big[\sum_a R^*_{a,\alpha}(\mathbf{k}) L_{a,\beta}(\mathbf{k}') g_{\alpha\beta}(\mathbf{k} - \mathbf{k}') - \{R^*_{e,\alpha}(\mathbf{k}) L_{h,\beta}(\mathbf{k}') + R^*_{h,\alpha}(\mathbf{k}) L_{e,\beta}(\mathbf{k}')\} g_{\alpha\beta}(\mathbf{k} - \mathbf{k}' - \mathbf{Q}) \Big] + \text{H.c.} \tag{74}$$

The value of the coupling constant γ can be extracted from Eqs. (42) and (76) by noting that it is this interaction which gives rise to the logarithmic singularity in $J(Q)$,

$$\tilde{J}^{\rm sing}(0,0,\mathbf{Q}) \approx -2\gamma^2 m^2 \frac{\rho(0)}{a_0} \ln\left[\frac{\delta t}{T}\right]. \tag{75}$$

Here $\rho(0)$ is the density of states per species at the Fermi surface of coherent fermions,

$$\rho(0) = \lim_{\omega \to 0} a_0 \int \frac{d^3\mathbf{k}}{(2\pi)^3} \left[-\frac{1}{\pi} \text{Im}\, G(\omega, k_F + q, \mathbf{k}_\perp) \right] \approx 0.539 \frac{a_0}{(2\pi)^2} \frac{\kappa_0^2}{v} \left[\frac{\delta t}{t_0}\right]^{1/2}. \tag{76}$$

The result is that close to the transition we have

$$\gamma \propto \sqrt{\frac{t}{m}}, \tag{77}$$

where $t \gg m$ is the hopping along the chains, and the constant of proportionality is of order 1. Though γ is never small, the small parameter κ_0^2 appears every time one integrates it over the transverse momentum. Hence the magnitude of γ is not a problem. The effective action describing the metallic side of the Mott-insulator to metal transition is given by Eqs. (57), (69), and (74). We find it instructive to write it down also in position space,

$$S_f = \int d\tau d^3\mathbf{x} \Psi^\dagger_\alpha(\tau,\mathbf{x}) \times \left\{ (I \otimes I)\partial_\tau + (I \otimes \tau^z) \left[E_0 + \frac{\partial_x^2}{2M_\parallel} + \frac{\vec{\nabla}_\perp^2}{2M_\perp} \right] \right\} \Psi_\beta(\tau,\mathbf{x}),$$

$$S_{\rm int} = \frac{\gamma m}{2} \int d\tau d^3\mathbf{x} \Psi^\dagger_\alpha(\tau,\mathbf{x}) (\{\tau^+ \otimes [\exp(-2iq_0 x \tau^z) - \tau^x \exp(-i\mathbf{Q}\cdot\mathbf{x}_\perp)]\} g_{\alpha\beta}(\tau,\mathbf{x}) + \text{H.c.}) \Psi_\beta(\tau,\mathbf{x}). \tag{78}$$

Here we have taken the continuum limit in the directions perpendicular to the chains and introduced a field $\Psi^+_\alpha = (\phi^* R^+_{e,\alpha}, \phi R^+_{h,\alpha}, \phi L^+_{e,\alpha}, \phi^* L^+_{h,\alpha})$, where $\phi = \exp(iq_0 x)$. We employ a tensor-product notation, where the first space is associated with the "right and/or left" index and the second space with the "e and/or h" index. The Fermi surfaces of electrons and holes are shifted to the origin and superimposed. The spin action $S[g]$ is given by Eq. (57). Alternatively, one may use the Abelian representation given by Eq. (9), with g defined by (15).

Marginal Fermi liquid

As we shall now demonstrate, at temperatures higher than the Néel temperature T_c this metal is, in fact a marginal

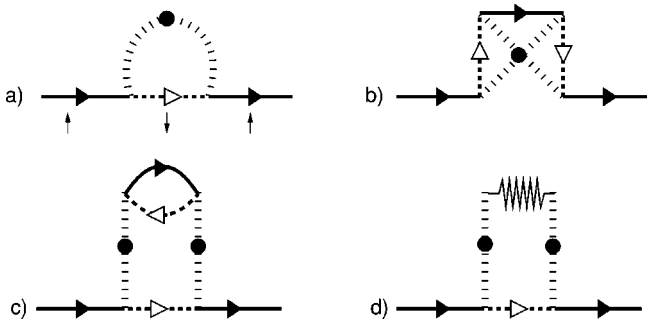

FIG. 7. Diagrams for the quasiparticle self-energy of right-moving electrons. The lines with arrows represent the fermionic Green's functions of right-moving and left-moving electrons and holes. The $2n$-point vertices denote cumulants of the matrix fields g and $g^{\dagger}$.

Fermi liquid.[18] The following discussion closely parallels the analysis given by Chubukov *et al.* for the spin-fermion model (see, for example Ref. 2). Let us consider the diagrams for the Green's function of right-moving electrons. We expand around uncoupled chains and take both the spin-fermion coupling and interchain spin-spin exchange into account, perturbatively. The elements of the diagram technique for the fermionic degrees of freedom are as usual, whereas the building blocks in the spin sector are the connected $2n$-point spin correlators for a single chain. In diagrams that do not contain closed fermionic loops or the interchain exchange such as the ones in Figs. 7(a) and 7(b), the spin correlations are independent of the transverse wave vector. This means that each fermion Green's function is integrated over $k_{\perp}$. This integral does not differ significantly from the integral over all momenta and as a result is independent of $q_{\parallel}$, corresponding to a Green's function that is local in real space,

$$\frac{\mathrm{d}\mathbf{k}_{\perp}^2}{(2\pi)^2}\frac{1}{\mathrm{i}\omega - E_e^L(q,\mathbf{k}_{\perp})} \approx \mathrm{const}\,\mathrm{i}\kappa_0^2\,\mathrm{sgn}(\omega). \tag{79}$$

As (79) is independent of q, we may integrate the spin correlator in the diagram of Fig. 7(a) over q. This makes the spin correlator local. As a result the contributions to the self-energy that do not contain closed fermionic loops or interchain spin exchange are approximately momentum independent. Then the self-energy calculation becomes essentially a local problem, such as the problem of electron-phohon interactions in metals and superconductors (the Eliashberg theory).[19] In fact, such an approach works under less stringent conditions, namely, when the spin excitations in the transverse direction are much slower than the quasiparticles. Therefore the diagrams generating a $\mathbf{k}_{\perp}$ dependence of the spin-spin correlators, such as the ones in Figs. 7(c) and 7(d) do not affect the result for the electron self-energy, even close to the transition. Once such diagrams are neglected, we get an expansion where a factor κ_0^2 is associated with each fermionic line [originating from the integration over $\mathbf{k}_{\perp}$, as in Eq. (79)]. Since Σ depends only on frequency, making these lines fat does not change the result (79), and no self-consistency is required. The contribution from the diagram in Fig. 7(a) contains the correlation function,

$$\langle\langle e^{(i/2)\Theta(\tau_1)}e^{-(i/2)\Theta(\tau_2)}\rangle\rangle \simeq \frac{\left(\ln\left[\frac{\Lambda}{T}\right]\right)^{1/2}\pi T v^{-1}}{|\sin(\pi T[\tau_1-\tau_2])|}. \tag{80}$$

The contribution of the diagram in Fig. 7(a) to the self-energy is then

$$\Sigma^{(a)}(\omega) \propto \kappa_0^2\left(\ln\left[\frac{\Lambda}{T}\right]\right)^{1/2}\int \mathrm{d}\tau\frac{\mathrm{e}^{i\omega\tau}T}{\tau|\sin(\pi T\tau)|} \sim i\kappa_0^2\omega\ln\left[\frac{E_0}{\max\{\omega,T\}}\right]\left(\ln\left[\frac{\Lambda}{T}\right]\right)^{1/2}. \tag{81}$$

Here E_0^{-1} serves as a short-time cutoff in all integrals. The diagram in Fig. 7(b) involves cumulants of the type,

$$\langle\langle e^{(i/2)\Theta(\tau_1)}e^{-(i/2)\Theta(\tau_2)}e^{(i/2)\Theta(\tau_3)}e^{-(i/2)\Theta(\tau_4)}\rangle\rangle, \tag{82}$$

and gives a contribution,

$$\Sigma^{(b)}(\omega) \propto \kappa_0^6\int d\tau_2 d\tau_3 d\tau_4\frac{e^{i\omega\tau_{14}}}{\tau_{12}\tau_{23}\tau_{34}}\times\left[\left|\frac{\tau_{13}\tau_{24}}{\tau_{12}\tau_{14}\tau_{23}\tau_{34}}\right| - \frac{1}{|\tau_{12}\tau_{34}|} - \frac{1}{|\tau_{14}\tau_{23}|}\right] \propto \omega^2, \tag{83}$$

to the self-energy. Various other contributions are zero because some local cumulants vanish,

$$\langle\langle e^{(i/2)\Phi(\tau_1)}e^{-(i/2)\Theta(\tau_2)}e^{(i/2)\Theta(\tau_3)}e^{-(i/2)\Phi(\tau_4)}\rangle\rangle = 0. \tag{84}$$

Equation (83) shows that contributions from higher cumulants can be neglected at small frequencies. As a result, the only essential contribution to the self-energy comes from the diagram in Fig. 7(a) and is given by Eq. (81).

VI. THE ORDERED STATE

As we have discussed in the previous sections, the system undergoes an antiferromagnetic transition at a temperature much smaller than the Mott-Hubbard gap $T_c \sim m\kappa_0^2$. Once T_c becomes small, compared to the quasiparticle Fermi energy E_0, one can distinguish between metallic and insulating behavior. As we have demonstrated, the corresponding metal is rather unusual, being in fact a marginal Fermi liquid. Below T_c, however, the system becomes either an insulator (for zero doping) or an ordinary Fermi liquid. Indeed, at zero doping the electron and hole Fermi surfaces are nested, and the ordering occurs at the antiferromagnetic wave vector in the transverse direction (recall that the chains run along the z axis) such that

$$\langle g_{\mathbf{l},\alpha\beta}(x)\rangle = \vec{\sigma}_{\alpha\beta}\cdot\mathbf{M}(-1)^{l_x+l_y}. \tag{85}$$

Here the components of $\vec{\sigma}$ are the Pauli matrices and $\mathbf{M}$ is the ordering vector. In the mean-field approximation the fermionic spectrum is gapped,

$$\omega_a^2 = [E_a^R(\mathbf{k})]^2 + \gamma^2 m^2|\mathbf{M}|^2, \quad a = e,h. \tag{86}$$

At nonzero doping our approach still holds, provided the chemical potential lies inside the Mott-Hubbard gap. There is

no nesting any longer, and the magnetic ordering does not open a gap in the quasiparticle spectrum. As usual, the magnetic fluctuations interact with quasiparticles through gradient vertices, and these interactions are weak.

VII. CONCLUSIONS

The main result of this paper is a formulation of a self-consistent description of the hybrid state of 3D quasiparticles interacting with magnetic collective modes. The derivation is done for a toy model of half-filled Hubbard chains weakly coupled through a long-range interchain hopping. A certain artificiality of the model is necessary to ensure the self-consistency of our approach through the presence of a small parameter κ_0^2. We also neglect the long-range component of the Coulomb interaction, which plays an important role in determining the character of the metal-insulator transition. In reality a long-range interaction may lead to an instability of the small FS phase, though for a small Mott-Hubbard gap its influence is diminished by the presence of a large dielectric constant. In this case the first-order MI transition line may terminate below the antiferromagnetic transition line of Fig. 1.

The resulting low-energy effective theory is of the Eliashberg type: the interaction between quasiparticles and collective modes leads to strong retardation effects, resulting in a strongly frequency-dependent, quasiparticle self-energy. In the present model this takes place not just at the "hot spots" as in the spin-fermion model of Chubukov, Pines, and Schmalian, but on the entire quasiparticle FS. This makes the present model a candidate for the description of bad metals. The fact that in our model the electron self-energy is of the marginal Fermi liquid form is not universal and is determined by the particular spin-fluctuation spectrum.

As we discussed in the Introduction, our theory provides an example of a state where the number of carriers is unrelated to the volume of the FS. Though this idea is well established [see, e.g., the textbook (Ref. 5)], its microscopic realization was restricted to superconductors (the example given in Ref. 5). Our model provides another example. It also demonstrates that one does not need exotic ground states to have a small FS, as was suggested in Refs. 20 and 21. The small FS phenomenology can be generalized beyond our model. In general there is no *a priori* reason for the Fermi surface even to be closed; for instance, Ref. 22 describes a state with a truncated Fermi surface observed in ARPES experiments on undoped cuprates.[9]

ACKNOWLEDGMENTS

We are grateful to Andrei Chubukov for numerous discussions and interest in the work. A.M.T is grateful to S. Buehler-Paschen for information about Hall effect measurements. A.M.T. acknowledges support by the U. S. Department of Energy under Contract No. DE-AC02-98 CH 10886. F.H.L.E. is supported by the EPSRC under Grant No. GR/R83712/01 and the Institute for Strongly Correlated and Complex Systems at BNL.

[1] D. Pines, Z. Phys. B: Condens. Matter **103**, 129 (1997).
[2] A. Abanov, A. V. Chubukov, and J. Schmalian, Adv. Phys. **52**, 119 (2003); A. V. Chubukov, D. Pines, and J. Schmalian, cond-mat/0201140 (unpublished).
[3] F. H. L. Essler and A. M. Tsvelik, Phys. Rev. B **65**, 115117 (2002).
[4] J. M. Luttinger, Phys. Rev. **119**, 1153 (1960).
[5] A. A. Abrikosov, L. P. Gorkov, and I. E. Dzyaloshinski, *Methods of Quantum Field Theory in Statistical Physics* (Dover, New York, 1975) p. 168.
[6] I. E. Dzyaloshinski, Phys. Rev. B **68**, 085113 (2003).
[7] B. L. Altshuler, A. V. Chubukov, A. Dashevskii, A. M. Finkel'stein, and D. K. Morr, Europhys. Lett. **41**, 401 (1998).
[8] F. H. L. Essler and A. M. Tsvelik, Phys. Rev. Lett. **90**, 126401 (2003).
[9] M. R. Norman *et al.*, Nature (London) **392**, 157 (1998).
[10] S. Buehler-Paschen *et al.* (unpublished).
[11] S. Lukyanov and A. B. Zamolodchikov, Nucl. Phys. B **607**, 437 (2001).
[12] M. Dzero and L. P. Gor'kov, Phys. Rev. B **69**, 092501 (2004).
[13] D. Boies, C. Bourbonnais, and A.-M. S. Tremblay, Phys. Rev. Lett. **74**, 968 (1995).
[14] V. Barzykin, J. Phys.: Condens. Matter **12**, 2053 (2000).
[15] H. J. Schulz and C. Bourbonnais, Phys. Rev. B **27**, 5856 (1983).
[16] M. Bocquet, F. H. L. Essler, A. M. Tsvelik, and A. Gogolin, Phys. Rev. B **64**, 094425 (2001); M. Bocquet, Phys. Rev. B **65**, 184415 (2002).
[17] V. Y. Irkhin and A. A. Katanin, Phys. Rev. B **61**, 6757 (2000).
[18] C. M. Varma, P. B. Littlewood, S. Schmitt-Rink, E. Abrahams, and A. E. Ruckenstein, Phys. Rev. Lett. **63**, 1996 (1989).
[19] G. M. Eliashberg, Sov. Phys. JETP **11**, 696 (1960); D. J. Scalapino in *Superconductivity*, edited by D. Parks (Dekker Inc., New York, 1969), Vol. 1, p. 449; F. Marsiglio and J. P. Carbotte, in *The Physics of Conventional and Unconventional Superconductors*, edited by K. H. Bennemann and J. B. Ketterson (Springer-Verlag, Berlin).
[20] T. Senthil, S. Sachdev, and M. Vojta, Phys. Rev. Lett. **90**, 216403 (2003).
[21] T. Senthil, M. Vojta, and S. Sachdev, Phys. Rev. B **69**, 035111 (2004).
[22] C. Honerkamp, M. Salmhofer, N. Furukawa, and T. M. Rice, Phys. Rev. B **63**, 035109 (2001).